

1 Cost-benefit analysis of coastal flood defence measures in the North 2 Adriatic Sea

3 Mattia Amadio¹, Arthur H. Essenfelder¹, Stefano Bagli², Sepehr Marzi¹, Paolo Mazzoli², Jaroslav Mysiak¹,
4 Stephen Roberts³

5 ¹ *Centro Euro-Mediterraneo sui Cambiamenti Climatici, Università Ca' Foscari Venezia, Italy*

6 ² *Gecosistema, Rimini, Italy*

7 ³ *The Australian National University, Canberra, Australia*

8 Abstract

9 The combined effect of extreme sea levels and land subsidence phenomena poses a major threat to coastal
10 settlements. Coastal flooding events are expected to grow in frequency and magnitude, increasing the
11 potential economic losses and costs of adaptation. In Italy, a large share of the population and economic
12 activities are located along the coast of the peninsula, although risk of inundation is not uniformly distributed.
13 The low-lying coastal plain of Northeast Italy is the most sensitive to relative sea level changes. Over the last
14 half a century, the entire north-eastern Italian coast has experienced a significant rise in relative sea level, the
15 main component of which was land subsidence. In the forthcoming decades, climate-induced sea level rise is
16 expected to become the first driver of coastal inundation hazard. We propose an assessment of flood hazard
17 and risk linked with extreme sea level scenarios, both under historical conditions and sea level rise projections
18 at 2050 and 2100. We run a hydrodynamic inundation model on two pilot sites located in the North Adriatic
19 Sea along the Emilia-Romagna coast: Rimini and Cesenatico. Here, we compare alternative risk scenarios
20 accounting for the effect of planned and hypothetical seaside renovation projects against the historical
21 baseline. We apply a flood damage model developed for Italy to estimate the potential economic damage
22 linked to flood scenarios and we calculate the change in expected annual damage according to changes in the
23 relative sea level. Finally, damage reduction benefits are evaluated by means of cost-benefit analysis. Results
24 suggest an overall profitability of the investigated projects over time, with increasing benefits due to increased
25 probability of intense flooding in the next future.

26 **Key-words:** coastal inundation Italy extreme sea level rise

27 **Abbreviations:** MSL (Mean Sea Level); TWL (Total Water Level); ESL (Extreme Sea Level); SLR (Sea Level
28 Rise); VLM (Vertical Land Movements); DTM (Digital Terrain Model); EAD (Expected Annual Damage)

29 1. Introduction

30 Globally, more than 700 million people live in low-lying coastal areas (McGranahan et al. 2007), and about
31 13% of them are exposed to a 100-year return period flood event (Muis et al. 2016). On average, one million
32 people located in coastal areas are flooded every year (Hinkel et al. 2014). Coastal flood risk shows an
33 increasing trend in many places due to socio-economic growth (Bouwer 2011; Jongman et al. 2012b) and land
34 subsidence (Syvitski et al. 2009; Nicholls and Cazenave 2010), but in the near future sea level rise (SLR) will
35 likely be the most important driver of increased coastal inundation risk (Hallegatte et al. 2013; Hinkel et al.
36 2014). Evidences show that global sea level has risen at faster rates in the past two centuries compared to the
37 millennial trend (Kemp et al. 2011; Church and White 2011), topping 3.2 mm per year in the last decades
38 mainly due to ocean thermal expansion and glacier melting processes (Mitchum et al. 2010; Meyssignac and
39 Cazenave 2012). According to the IPCC projections, it is very likely that, by the end of the 21st century, the
40 SLR rate will exceed that observed in the period 1971-2010 for all Representative Concentration Pathway (RCP)
41 scenarios (IPCC 2019); yet the local sea level can have a strong regional variability, with some places

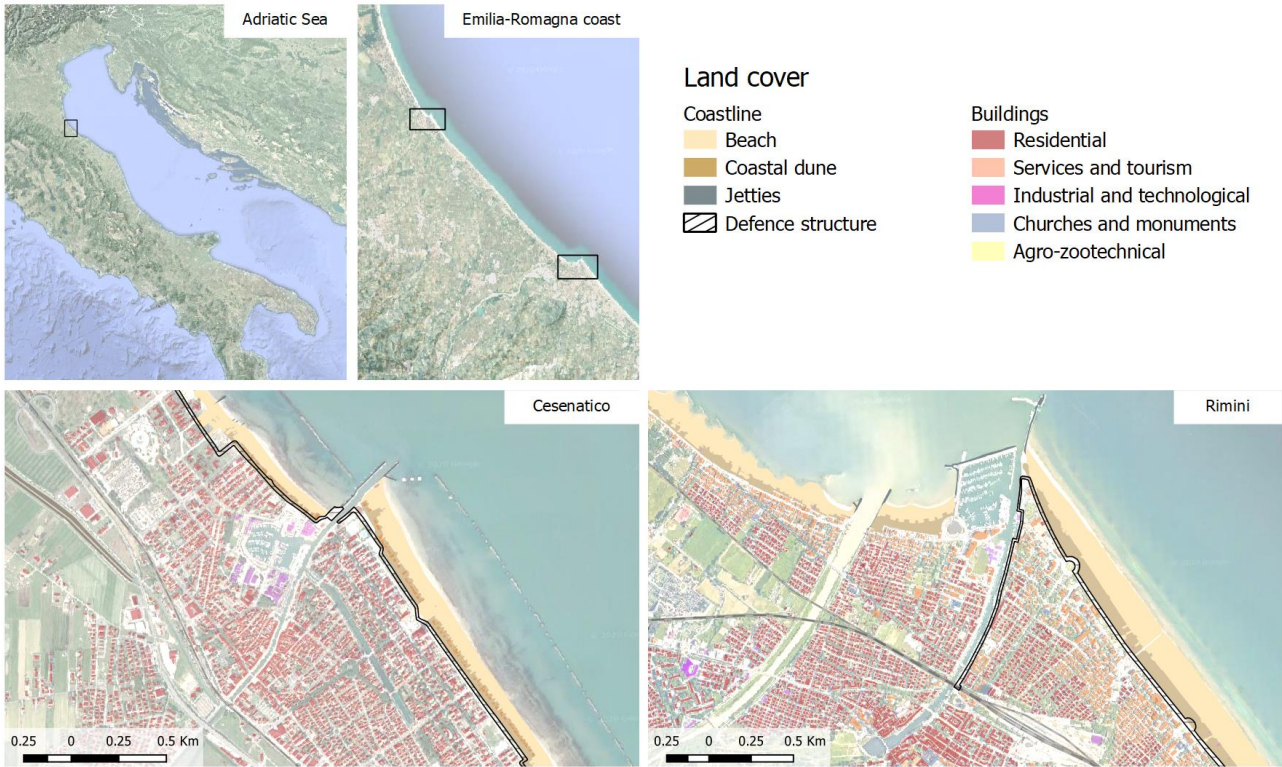
42 experiencing significant deviations from the global mean change (Stocker et al. 2013). This is particularly
43 worrisome in regions where changes in the mean sea level (MSL) are more pronounced, considering that even
44 small increases of MSL can drastically change the frequency of extreme sea level (ESL) events, leading up to
45 situations where a 100-year event may occur several times per year by 2100 (Carbognin et al. 2009, 2010;
46 Vousdoukas et al. 2017, 2018; Kirezci et al. 2020). Changes in the frequency of extreme events are likely to
47 make existing coastal protection inadequate in many places, causing a large part of the European coasts to be
48 exposed to flood hazard. Under these premises, coastal floods threaten to trigger devastating impacts on
49 human settlements and activities (Lowe et al. 2001; McInnes et al. 2003; Vousdoukas et al. 2017). In this context,
50 successful coastal risk mitigation and adaptation actions require accurate and detailed information about the
51 characterisation of coastal flood hazard and the performance of alternative coastal defence options. Cost-
52 benefit analysis (CBA) is widely used to evaluate the economic desirability of a disaster risk reduction (DRR)
53 project (Jonkman et al. 2004; Mechler 2016; Price 2018). CBA helps decision-makers in evaluating the efficacy
54 of different adaptation options (Kind 2014; Bos and Zwaneveld 2017).

55 In this study, we estimate the benefits of coastal renovation projects along the coast of Emilia-Romagna region
56 (Italy) in terms of avoided economic losses from ESL inundation events under both current and future
57 conditions. We select two coastal cities as case study areas: i) Rimini, a touristic hotspot that is currently
58 implementing a seafront renovation project; and ii) Cesenatico, a coastal city that could benefit from similar
59 measures in addition to existing defence mechanisms. We design worst-case scenarios of ESL resulting from
60 the combination of the maximum levels of mean sea level, vertical land movement, storm surge, tide, and
61 wave setup to verify the effectiveness of the above-mentioned coastal defence structures in reducing flood
62 hazard and related impacts over the urban area. To do that, first we employ the 2D-hydrodynamic ANUGA
63 model (Roberts et al. 2015) for simulating coastal inundation associated with ESL scenarios over the two case
64 study areas. The scenarios are calculated by combining probabilistic data from historical ESL events with the
65 estimates of relative mean sea level (RMSL) change for those locations. RMSL change accounts for both the
66 eustatic global rise and the locally-measured vertical land movement effect. Each inundation scenario
67 simulated by the hydrodynamic model is translated in terms of direct economic impacts over residential areas
68 using a locally-calibrated damage model. The combination of different risk scenarios in a CBA framework
69 allows to evaluate the economic benefits brought by the project implementation in terms of avoided direct
70 flood losses up to the end of the century.

71 **2. Area of study**

72 Located in the central Mediterranean Sea, the Italian peninsula has more than 8,300 km of coasts, hosting
73 around 18% of the country population, numerous towns and cities, industrial plants, commercial harbours
74 and touristic activities, as well as cultural and natural heritage sites. Existing country-scale estimates of SLR
75 impacts up to the end of this century helps to identify the most critically exposed coastal areas of Italy
76 (Lambeck et al. 2011; Bonaduce et al. 2016; Antonioli et al. 2017; Marsico et al. 2017). About 40% of the country's
77 coastal perimeter consist of a flat coastal profile (ISPRA 2012), potentially more vulnerable to the impacts of
78 ESL events. The North Adriatic coastal plain is acknowledged to be the largest and most vulnerable location
79 to extreme coastal events due to the shape, morphology and low bathymetry of the Adriatic sea basin, which
80 cause water level to increase relatively fast during coastal storms (Carbognin et al. 2010; Ciavola and Coco
81 2017; Perini et al. 2017). The ESL here is driven mainly by astronomical tide, ranging about one meter in the
82 northernmost sector; and meteorological forcing, such as low pressure, seiches and prolonged rotational wind
83 systems, which are the main trigger of storm surge in the Adriatic basin (Vousdoukas et al. 2017; Umgiesser
84 et al. 2020). In addition to that, all the coastal profile of the Padan plain shows relatively fast subsiding rates,

85 partially due to natural phenomena, but in large part linked to human activities (Carbognin et al. 2009; Perini
 86 et al. 2017; Meli et al. 2021). As a contributing factor to coastal flood risk, the intensification of urbanization
 87 has led to increased exposure along the Adriatic coast during the last 50 years, with many regions building
 88 over half of the available land within 300 meters from the shoreline (ISPRA 2012). Figure 1 shows the location
 89 of the two case study areas, Cesenatico and Rimini, along with land-cover maps showing the position of coastal
 90 defences accounted in this study.



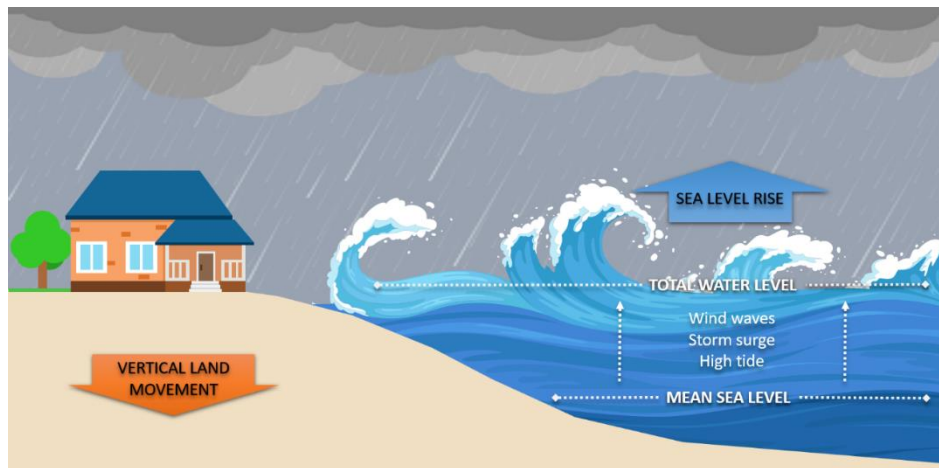
91
 92 **Figure 1.** Case-study locations along the Emilia-Romagna coast: Cesenatico and Rimini. The coastal defence
 93 structure assessed in this study are shown in black. Buildings' footprint data from Regional Environmental
 94 Agency (ARPA) 2020. Basemap © Google Maps 2020.

95 The number of ESL events reported to cause impacts along the Emilia-Romagna coast shows a steady increase
 96 since the second half of the past century (Perini et al. 2011), which is in part explained by to the socio-economic
 97 development of the coast exposing increasing asset to flood risk. The landscape along the 130 km regional
 98 coastline is almost flat, the only relief being old beach ridges, artificial embankments and a small number of
 99 dunes. The coastal perimeter is delineated by a wide sandy beach that is generally protected by offshore
 100 breakwaters, groins and jetties. The land elevation is often close to (or even below) the MSL, while the coastal
 101 corridor is heavily urbanised. Cesenatico has about 26,000 residents, while Rimini has 150,000. The towns have
 102 a strong touristic vocation, hosting large beach resort and bathing facilities along the beach and hundreds of
 103 hotels and rental housing located just behind the seaside. Both places have been affected by coastal storms
 104 resulting in flooding of buildings and activities, beach erosion and regression of the coastline. The most recent
 105 inundation events were observed in March 2010, November 2012 and February 2015. The 2015 event was one
 106 of the most severe ever recorded, with ESL values corresponding to a probability of once in 100 years. It caused
 107 severe damages along the whole regional coast and, in some locations, required the evacuation of people from
 108 their houses; many buildings and roads were covered by sand brought by the flood wave; touristic
 109 infrastructures near the shore were seriously damaged, and some port channels overflowed the surrounding
 110 areas. The economic impact of the event was estimated topping 7.5 M Eur (Perini et al. 2015).

111 3. Methodology

112 3.1 Components of the analysis

113 Coastal inundation is caused by an increase of total water level (TWL), most often associated to extreme sea
114 level (ESL) events, which are often generated by a combination of high astronomical tide and meteorological
115 drivers such as storm surge and wind waves (figure 2). Estimates of ESL are obtained for the North Adriatic
116 up to year 2100 by combining reference hazard scenarios derived from historical records with regionalised
117 projections of SLR (Vousdoukas et al. 2017) and local vertical land movements (VLM) rates (Carbognin et al.
118 2009; Perini et al. 2017). Four ESL frequency scenarios, namely once in 1, 10, 100 and 250 years, are considered.
119 The hydrodynamic model ANUGA is applied to simulate the inundation of land areas during ESL accounting
120 for individual components (storm surge, tides and waves). Land morphology and exposure of coastal
121 settlements are described by high-resolution DTM and bathymetry, in combination with land use and
122 buildings footprints. The effect of hazard mitigation structures (both designed and under construction) are
123 explicitly accounted in the “defended” simulation scenario, in contrast to the baseline scenario, where only
124 existing defence structures (groins, jetties, breakwaters and sand dunes) are accounted.



125
126 **Figure 2.** Components of the analysis for extreme sea level events: total water level is the sum of maximum
127 tide, storm surge and wind waves over mean sea level. Vertical land movement and eustatic sea level rise
128 affects the mean sea level on the long run.

129 3.2 Vertical Land Movement

130 Vertical land movements result from a combination of slow geological processes such as tectonic activity and
131 glacial isostatic adjustment (Peltier 2004; Peltier et al. 2015), and medium-term phenomena, such as sediment
132 loading and soil compaction (Carminati and Martinelli 2002; Lambeck and Purcell 2005). The latter can greatly
133 oversize geological processes at local scale (Wöppelmann and Marcos 2012); in particular, faster subsidence
134 occurs in presence of intense anthropogenic activities such as water withdrawal and natural gas extraction
135 (Teatini et al. 2006; Polcari et al. 2018). Most of the peninsula shows a slow subsiding trend, although with
136 some local variability. An estimate of VLM rates due to tectonic activity has been derived from studies
137 conducted in Italy (Lambeck et al. 2011; Antonioli et al. 2017; Marsico et al. 2017; Solari et al. 2018). The North
138 Adriatic coastal plain shows the most intense long-term geological subsidence rates (about 1 mm per year),
139 increasing North to South. Yet in the last decades these rates were often greatly exceeded by ground
140 compaction rates observed by multi-temporal SAR Interferometry (Gambolati et al. 1998; Antonioli et al. 2017;
141 Polcari et al. 2018; Solari et al. 2018). Observed subsidence is about one order of magnitude faster where the
142 aquifer system has been extensively exploited for agricultural, industrial and civil use since the post-war
143 industrial boom. From the 1970s, however, with the halt of groundwater withdrawals, anthropogenic drivers

144 of subsidence has been strongly reduced or stopped (Carbognin et al. 2009). Nonetheless, subsidence still
145 continues at much faster rates than expected from natural phenomena (Teatini et al. 2005). Geodetic surveys
146 carried out from 1953 to 2003 along the Ravenna coast provide evidence of a cumulative land subsidence
147 exceeding 1 m at some sites due to gas extraction activities. Average subsidence rates observed for 2006-2011
148 along the Emilia-Romagna coast are around 5 mm/yr, exceeding 10 mm/yr in the back shore of the Cesenatico
149 and Rimini areas and topping 20-50 mm/yr in Ravenna (Carbognin et al. 2009; Perini et al. 2017). Based on
150 these current rates, we assume an average fixed annual VLM of 5 mm in both Cesenatico and Rimini up to the
151 end of the century. This remarkable difference between natural VLM rates and observations would produce a
152 dramatic effect on the estimated SLR scenarios: at present rates, Rimini would see an increase of MSL by 0.15
153 m in 2050 and more than 0.4 m in 2100 independently from eustatic SLR. Since these rates are connected with
154 human activity, it is not possible to foresee exactly how they will change in the long term.

155 3.3 Sea Level Rise

156 The long availability of tide gauge data along the North Adriatic coast allows to assess the changes in MSL
157 during the last century. Records from the gauge station of Marina di Ravenna show an eustatic rise of 1.2 mm
158 per year from 1890 to 2007 (Meli et al. 2021), in good agreement with the eustatic rise measured at other stations
159 in the Mediterranean Sea (Tsimplis and Rixen 2002; Carbognin et al. 2009). The projections of future MSL
160 account for sea thermal expansions from four global circulation models, estimated contributions from ice-
161 sheets and glaciers (Hinkel et al. 2014) and long-term subsidence projections (Peltier 2004). The ensemble mean
162 is chosen to represent each RCP for different time slices. The increase in the central Mediterranean basin is
163 projected to be approximately 0.2 m by 2050 and between 0.5 and 0.7 m by 2100, compared to historical mean
164 (1970-2004) (Vousdoukas et al. 2017). As agreed with stakeholders, our analysis considers the intermediate
165 emission scenario RCP 4.5, projecting an increase in MSL of 0.53 m at 2100. It must be noted that these
166 projections, although downscaled for the Adriatic basin, do not account for the peculiar continental
167 characteristics of the shallow northern Adriatic sector, where the hydrodynamics and oceanographic
168 parameters partially depend on the freshwater inflow (Zanchettin et al. 2007).

169 3.4 Tides and meteorological forcing

170 Storm surge and wind waves represent the largest contribution to TWL during an ESL event. An estimation
171 of these components is obtained for the two coastal sites from the analysis of tide gauge and buoy records,
172 and from the description of historical extreme events presented in local studies (Perini et al. 2011, 2012, 2017;
173 Masina et al. 2015; Armaroli and Duo 2018). This area is microtidal: the mean neap tidal range is 30–40 cm,
174 and the mean spring tidal range is 80–90 cm. Most storms have a duration of less than 24 h and a maximum
175 significant wave height of about 2.5 m. During extreme cyclonic events, the sequence of SE wind (*Sirocco*)
176 piling the water North and E-NE wind (*Bora*) pushing waves towards the coast can generate severe inundation
177 events, with significant wave height ranging 3.3 – 4.7 m and exceptionally exceeding 5.5 m (Armaroli et al.
178 2012). Fifty significant events have been recorded from 1946 to 2010 on the ER coast, with half of them causing
179 severe impacts along the whole coast and 10 of them being associated with important flooding events (Perini
180 et al. 2017). The most severe events are found when strong winds blow during exceptional tide peaks, most
181 often happening in late autumn and winter. The event of November 1966 represents the highest ESL on
182 records, causing significant impacts along the regional coast: the recorded water level was 1.20 m above MSL,
183 and wave heights offshore were estimated around 6–7 m (Perini et al. 2011; Garnier et al. 2018). The whole
184 coastline suffered from erosion and inundation, especially in the province of Rimini. Atmospheric forcing
185 shown significant variability for the period 1960 onwards (Tsimplis et al. 2012), but there is no strong evidence

186 supporting a significant change in trend for the next future (Lionello 2012; Lionello et al. 2020; Zanchettin et
187 al. 2020). Thus, we assume the frequency and intensity of meteorological events to remain the same up to 2100.

188 3.5 Terrain morphology and coastal defence structures

189 Reliable bathymetries and topography are required in order to run the hydrodynamic modelling at the local
190 scale. Bathymetric data for the Mediterranean Sea were obtained from the European Marine Observation and
191 Data Network (EMODnet) at 100 m resolution. The description of terrain morphology comes from the official
192 high-resolution LIDAR DTM (MATTM, 2019). First, we combined the coastal dataset (2 m resolution and
193 vertical accuracy of ± 0.2 m), and the inland dataset (1 m resolution and vertical accuracy ± 0.1 m) into one
194 seamless layer. Then, the DTM is supplemented with geometries of existing coastal protection elements such
195 as jetties, groins and breakwaters obtained from the digital Regional Technical Map. In Rimini, the *Parco del*
196 *Mare* (figure 3) is an urban renovation project which aims to improve the seafront promenade: the existing
197 road and parking lots are converted into an urban green infrastructure consisting of a concrete barrier covered
198 by vegetated sandy dunes with walking paths. This project also acts as a coastal defence system during
199 extreme sea level events. The barrier rises 2.8 meters along the southern section of the town, south of the
200 marina; no barrier is planned on the northern coastal perimeter. The *Parco del Mare* project is currently under
201 construction and has been taken in account in the evaluation of the “defended” scenarios by adding the barrier
202 to the DTM.



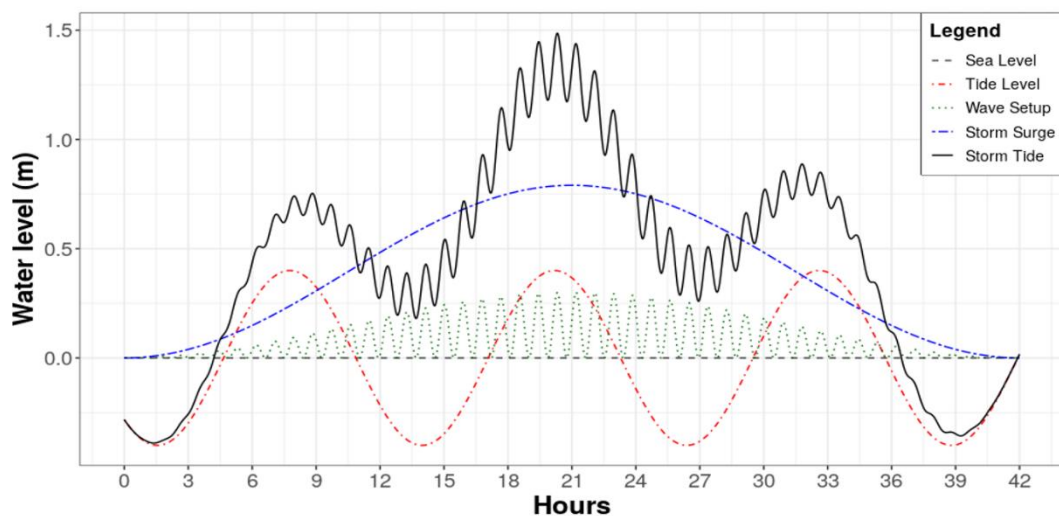
203
204 **Figure 3.** Prototype design of Parco del Mare project in Rimini. Adapted from JDS Architects.

205 In Cesenatico, the existing defence structures include a moving barrier system (*Porte Vinciane*) located on the
206 port channel, coupled with a dewatering pump which discharge the meteoric waters in the sea. The barriers
207 close automatically if the TWL surpasses 1 meter over the mean sea level, preventing floods in the historical
208 centre up to 2.2 meters of TWL. Additional defence structures include the winter dunes, which consist of a 2.2
209 meter-tall intermittent, non-reinforced sand barrier. In the defended scenario, we envisage a coastal defence
210 structure similar to Rimini’s *Parco del Mare* project, spanning both North and South of the port channel with a
211 total length of 7.8 km. A proper setup of the inundation model required to first perform some manual editing
212 of the DTM using additional reference data (i.e. on-site observations or aerial photography) in order to
213 produce an elevation model that realistically represent the land morphology and associated water dynamics
214 (e.g. removal of non-existent sink holes). Bridges and tunnels are the most critical elements that required DTM
215 correction in order to avoid misrepresentations of the water flow routing.

216 3.6 Inundation modelling

217 At the local scale, hydrodynamic models represent an efficient compromise between hydrostatic and hydraulic
218 models, being able to perform realistic simulations of inundation phenomena and to obtain detailed
219 information about the hazard features, while requiring a relatively fast setup and reasonable computational

220 effort. In this study we use ANUGA, a 2D hydrodynamic model originally developed to simulate tsunami
 221 events, which is also suitable for the simulation of hydrologic phenomena such as riverine peak flows and
 222 storm surges (Roberts 2020). Being a 2D hydrodynamic model, ANUGA does not resolve vertical convection,
 223 waves breaking or 3D turbulence (e.g. vorticity), thus it does not account for the swash component of wave
 224 runup. The fluid dynamics in ANUGA is based on a finite-volume method for solving the shallow water wave
 225 equations, thus being based on continuity and simplified momentum equation. The model computes the total
 226 water level, the water depth, and the horizontal momentum on an irregular triangular grid based on the
 227 provided forcing conditions. ANUGA includes also an operator module that simulates the removal of sand
 228 associated with over-topping of a sand dune by sea waves, which is applied to explore scenarios where a sand
 229 dune barrier provides protection for the land behind. The operator simulates the erosion, collapse, fluidisation
 230 and removal of sand from the dune system (Kain et al. 2020); the dune erosion mechanism relies on a
 231 relationship based on Froehlich (2002). This option is enabled only in the undefended scenario for Cesenatico,
 232 where non-reinforced sand dunes are prone to erosion.



233
 234 **Figure 4.** Total Water Level (black) as a sum of tide (red), storm surge (blue) and wave setup (green) for ESL
 235 scenario 1 in 10 years.

236 In our application, we estimate the TWL on the coastland at every timestep as the sum of extreme values for
 237 storm surge level (SS), wave setup (Ws), and max tide (T_{max}), as shown in figure 4. Storm surge peak is set to
 238 coincide with the tidal peak at the mid of the event, thus producing a maximum TWL value. As considered,
 239 our approach is precautionary as it provides worst-case scenario ESL values. The components of TWL are
 240 obtained from existing probabilistic analysis of extreme events conducted on the regional coast (Perini et al.
 241 2016, 2017) and later adopted by the Regional Environmental Agency to define the official coastal flood hazard
 242 zones (ARPAE 2019). The probability of occurrence for ESL scenarios is expressed in terms of return period
 243 (RP), which is the estimated average time interval between events of similar intensity, accounting for all
 244 variables combined. The maximum tidal excursion is 0.8-0.9 m, while wave setup near the shore can range
 245 from 0.22 to 0.65 m. For RP 250, TWL hits 2.5 meters as all components reach their most extreme values.
 246 Additional details are wave period (Wp , in seconds) and event duration ($Time$, in hours), required for the
 247 hydrodynamic simulation of coastal flooding events and the determination of the maximum extent of inland
 248 water propagation. Both variables are obtained from existing analysis of historical ESL events records matched
 249 with the probabilistic distribution of RP scenarios (Armaroli et al. 2012; Armaroli and Duo 2018). In our
 250 scenarios, wave direction is set to be oriented perpendicular to the coast. Table 1 summarizes the ESL
 251 components according to the four probability scenarios identified from local historical records (Perini et al.

252 2017). The output of the simulation consists of maps representing flood extent, water depth and momentum
 253 at every time step (1 second), projected on the high-resolution DTM grid.

254 **Table 1.** components of TWL during an ESL event under historical conditions and projected conditions (2050
 255 and 2100), accounting for both eustatic SLR (RCP 4.5) and average VLM rate.

RP (years)	Extreme event features				Historical	2050			2100		
	SS (m)	Tmax (m)	Ws (m)	Time (h)	TWL (m)	SLR (m)	VLM (m)	TWL (m)	SLR (m)	VLM (m)	TWL (m)
1	0.60	0.40	0.22	32	1.2	0.14	0.19	1.55	0.53	0.44	2.2
10	0.79	0.40	0.30	42	1.5	0.14	0.19	1.82	0.53	0.44	2.5
100	1.02	0.40	0.39	55	1.8	0.14	0.19	2.14	0.53	0.44	2.8
250	1.40	0.45	0.65	75	2.5	0.14	0.19	2.83	0.53	0.44	3.5

256 3.7 Risk modelling and Expected Annual Damage

257 Direct damage to physical asset is estimated using a customary flood risk assessment approach originally
 258 developed for fluvial inundation, which is adapted to coastal flooding assuming that the dynamic of impact
 259 from long-setting floods depends on the same factors, namely: 1) hazard magnitude, and 2) size and value of
 260 exposed asset. Indirect economic losses due to secondary effects of damage (e.g. business interruption) are
 261 excluded from the computation. Hazard magnitude can be defined by a range of variables, but the most
 262 important predictors of damage are water depth and the extension of the flood event (Jongman et al. 2012a;
 263 Huizinga et al. 2017). Land cover definitions and buildings footprints help to estimate the exposed capital
 264 including residential buildings, commercial and industrial activities, infrastructures, historical and natural
 265 sites. The characterization of exposed asset is built from a variety of sources, starting from land use and
 266 buildings footprints obtained from the Regional Environmental Agencies geodatabases and the Open Street
 267 Map database (Geofabrik GmbH 2018). Additional indicators about buildings characteristics are obtained
 268 from the database of the 2011 Italian Census (ISTAT 2011), while mean construction and restoration costs per
 269 building types are obtained from cadastral estimates (CRESME 2014). The asset representation is static, thus
 270 not accounting for changes in land use nor population density, while allowing for the direct comparison of
 271 hazard mitigation options' results. A depth-damage function was previously validated on empirical records
 272 (Amadio et al. 2019) and then applied in order to translate each hazard scenario into an estimate of economic
 273 risk, measured as a share of total exposed value. The damage function applies only to residential and mixed-
 274 residential buildings, the area of which represents about 93% of total exposed footprints; other types (such as
 275 harbour infrastructures, industrial, commercial, historical monuments and natural sites) are excluded from
 276 risk computation. Abandoned or under-construction buildings are also excluded from the analysis. To avoid
 277 overcounting of marginally-affected buildings, we set two threshold conditions for damage calculation: flood
 278 extent must be greater than or equal to 10 m², and maximum water depth greater than or equal to 10 cm. The
 279 damage/probability scenarios are combined together as Expected Annual Damage (EAD). EAD is the damage
 280 that would occur in any given year if damages from all flood probabilities were spread out evenly over time;
 281 mathematically, EAD is the integration of the flood risk density curve over all probabilities (Olsen et al. 2015),
 282 as in equation 1.

$$EAD = \int_0^1 D(p) dp \quad (1)$$

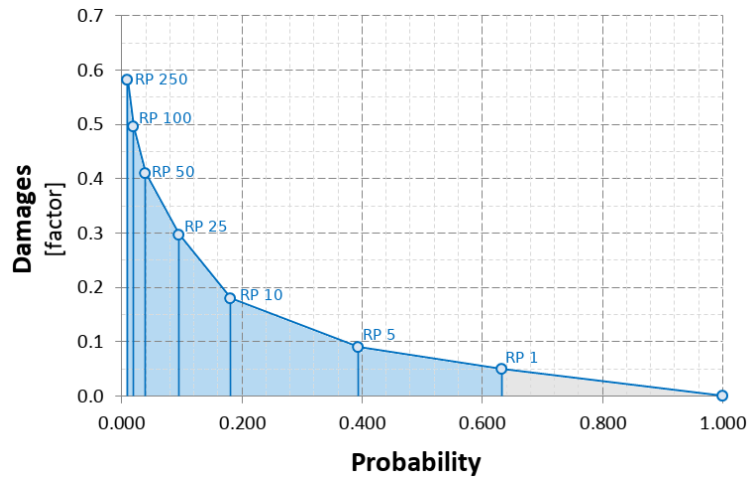
283 The integration of the curve can be solved either analytically or numerically, depending on the complexity of
 284 the damage function $D(p)$. Several different methods for numerical integration exist; we use an approach
 285 where EAD is the sum of the product of the fractions of exceedance probabilities by their corresponding

286 damages (figure 5). We calculate $D(p)$, which is the damage that occurs at the event with probability p , by
 287 using the depth-damage function for each hazard scenario. The exceedance probability of each event (p) is
 288 calculated based on exponential function as shown in equation 2.

$$p = 1 - e^{\left(\frac{-1}{RP}\right)} \quad (2)$$

289 Events with a high probability of occurrence and low intensity (below RP 1 year) are not simulated, as they
 290 are assumed to not cause significant damage. This is consistent with the historical observations for the case
 291 study area, although this assumption could change with increasing MSL.

Figure 5. Schematic representation of the numerical integration of the damage function $D(p)$ with respect to the exponential probability of the hazard events. Events with a probability of occurrence higher than once in a year are expected to not cause damage (grey area).



292 3.8 Cost-Benefit Analysis

293 A CBA should include a complete assessment of the impacts brought by the implementation of the hazard
 294 mitigation option, i.e. direct and indirect, tangible and intangible impacts (Bos and Zwaneveld 2017). The
 295 project we are considering, however, has not been primarily designed for DRR purpose: instead, it is meant
 296 as an urban renovation project which aims to consolidate the touristic vocation of the area, to improve the
 297 quality of life and the urban environment (Comune di Rimini 2018). This implies some large indirect effects
 298 on the whole area, most of which are not strictly related to disaster risk management and, overall, very difficult
 299 to estimate ex-ante. Our evaluation focuses only on the benefits that are measurable in terms of direct flood
 300 losses reduction. Regarding the implementation costs, the CBA accounts for the initial investment required
 301 for setting up the adaptation measure, and operational costs through time. According to the *Parco del Mare*
 302 project funding documentation (Comune di Rimini 2019a, b, 2020, 2021a, b), the total cost of the project (to be
 303 completed during 2021) is 33.3 M Eur, corresponding to 5.55 M Eur per Km of length. No information is
 304 available about maintenance costs of the opera, but given the nature of the project (static defense with low
 305 structural fragility), we assume they will be rather small compared to the initial investment. Ordinary annual
 306 maintenance costs are accounted as 0.1% of the total cost of the project. The same costs are assumed for the
 307 hypothetical barrier in Cesenatico, resulting in an initial investment cost of 43.3 M. Costs and benefit occurring
 308 in the future periods need to be discounted, as people put higher value on the present (Rose et al., 2007). This
 309 is done by adjusting future costs and benefits using an annual discount rate (r). We chose a variable rate of $r =$
 310 3.5 for the first 50 years and $r = 3$ from 2050 onward (Lowe 2008). A sensitivity analysis of discount rate is
 311 included in Annex 1. The three main decision criteria used in CBA for project evaluation are the Net Present
 312 Value (NPV), the Benefit/Cost Ratio (BCR) and the payback period. The NPV is the sum of Expected Annual
 313 Benefits (B) up to the end of the time horizon, discounted, minus the total costs for the implementation of the
 314 defense measure, which takes into account initial investment plus discounted annual maintenance costs (C).

315 In other words, the NPV of a project equals the present value of the net benefits ($NB_i = B_i - C_i$) over a period of
316 time (Boardman et al. 2018), as in equation (3):

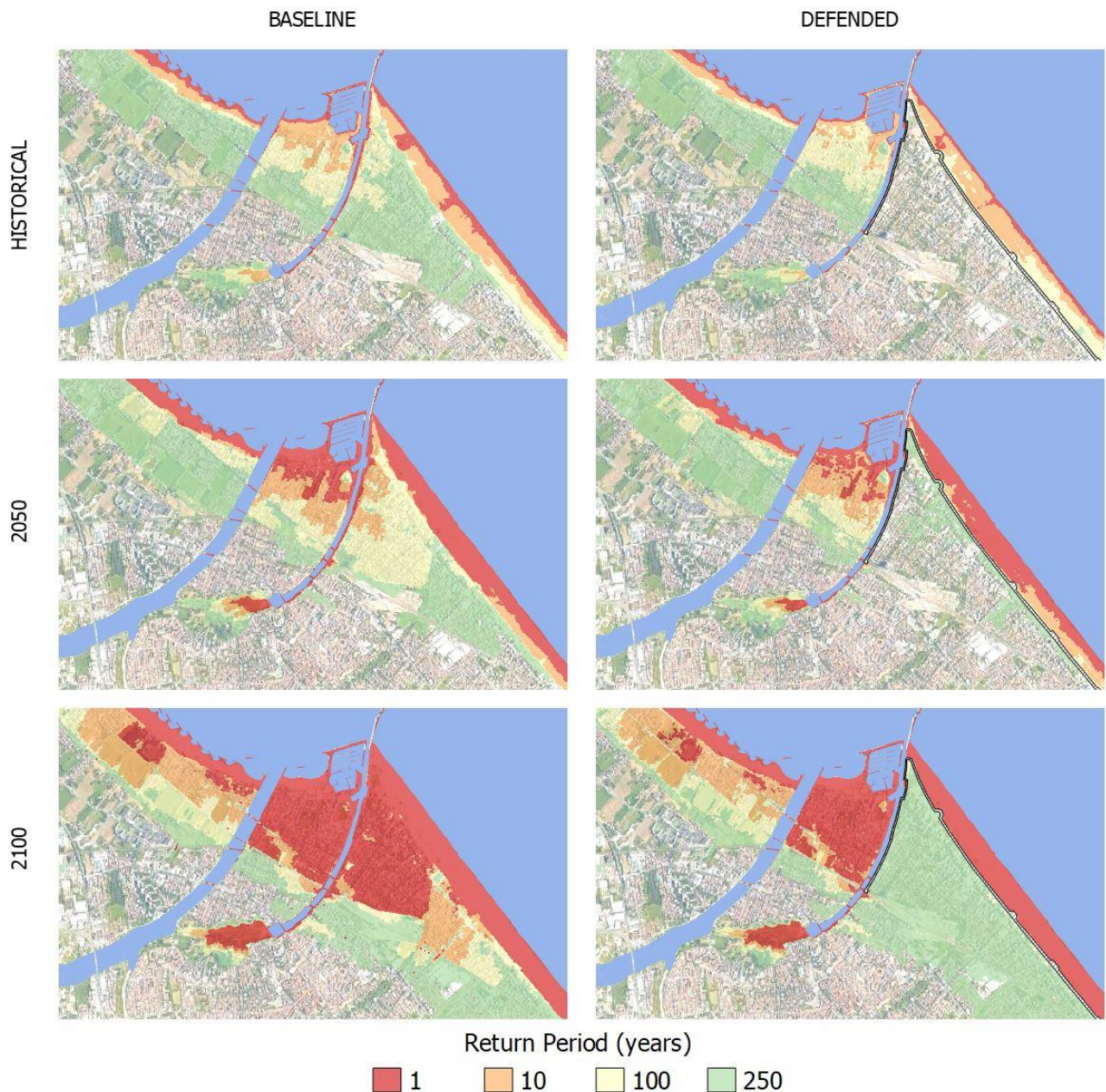
$$NPV = PV(B) - PV(C) = \sum_{t=0}^n \frac{NB_t}{(1+r)^t} \quad (3)$$

317 Positive NPV means that the project is economically profitable. The BCR is instead the ratio between the
318 benefits and the costs; a BCR larger than 1 means that the benefits of the project exceed the costs on the long
319 term and the project is considered profitable. The payback period is the number of years required for the
320 discounted benefits to equal the total costs.

321 4. Results

322 4.1 Inundation scenarios

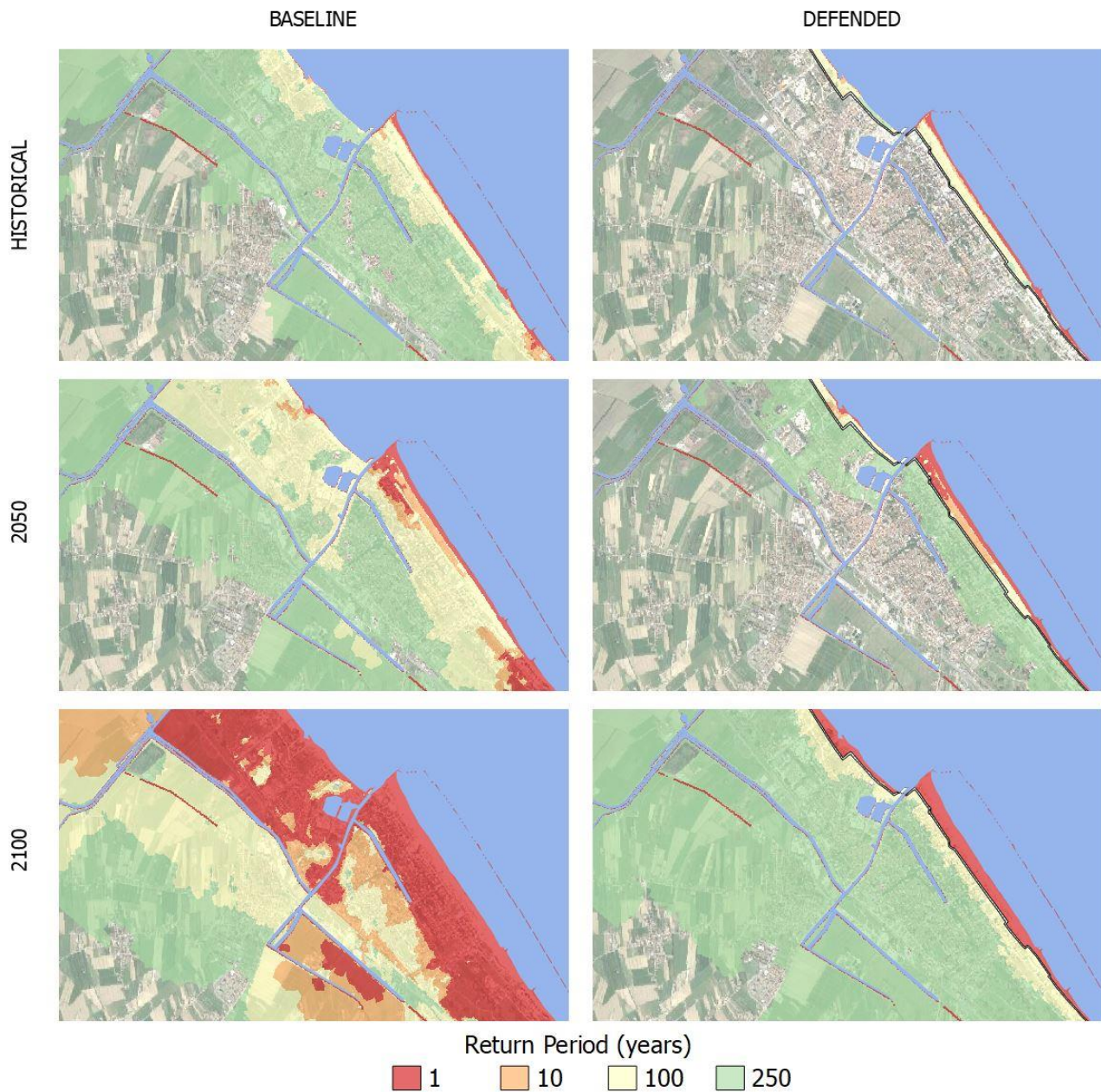
323 Once the setup is completed, the hydrodynamic model performs relatively fast: each simulation is carried at
324 half speed compared to real time, requiring about 24 hours to simulate a 12 h event. Parallel simulations for
325 the same area can run on a multicore processor, improving the efficiency of the process. The output of the
326 hydrodynamic model consists of a set of inundation simulations that include several hazard intensity variables
327 in relation to flood extent: water depth, flow velocity, and duration of submersion. ESL scenarios are then
328 summarized into static maps, each one representing the maximum value reached by hazard intensity variables
329 during the simulated event at about 1 meter resolution. The flood extents corresponding to each RP scenario
330 are shown for Rimini (figure 6) and Cesenatico (figure 7).



331

332 **Figure 6.** Rimini, extent of land affected by flood according to frequency of occurrence of ESL event up to 2100
 333 for the baseline [left] and the defended scenario [right]. Basemap © Google Maps 2020.

334 In Rimini, the *Parco del Mare* barrier produces benefits in terms of avoided damage in the south-eastern part
 335 of the town (high-density area) for ESL events with a return period of 100 years or less. The north-western part
 336 and the marina are outside of the defended area; these areas are therefore subject to a similar amount of
 337 flooding across scenarios. In all the simulations, the buildings located behind the marina are the firsts to be
 338 flooded. In fact, the new and the old port channels located on both sides of the marina represent a hazard
 339 hotspot: as shown in the maps, the failure of the eastern channel, which has a relatively low elevation, is likely
 340 to cause the water to flood the eastern part of the town, even during inundation events that would not surpass
 341 the beach. In the defended scenarios, where both the coastal and the canal barriers are enabled, the flood extent
 342 in the south-eastern urban area becomes almost zero for ESL events with a probability of once in 100 years,
 343 even when accounting for SLR up to 2100. Under the most exceptional ESL conditions (RP 250 in 2100), the
 344 barrier is overtopped, generating a flood extent similar to the baseline scenario for the same occurrence
 345 probability.



346

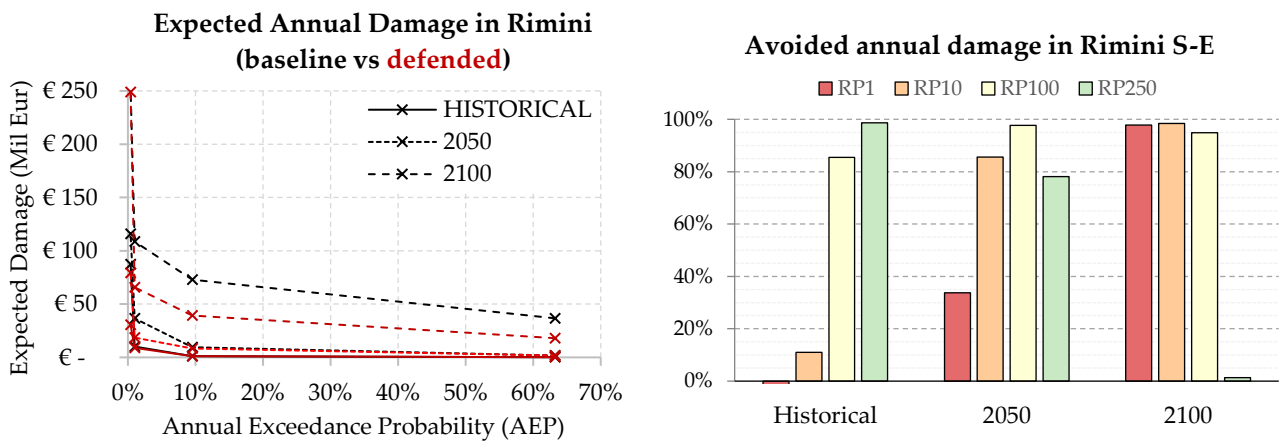
347 **Figure 7.** Cesenatico, extent of land affected by flood according to frequency of occurrence of ESL event up to
 348 2100 for the baseline [left] and the defended scenario [right]. Basemap © Google Maps 2020.

349 In Cesenatico, a barrier designed similarly to *Parco del Mare* could provide significant reduction of flood extents
 350 under most hazard scenarios. Its effectiveness would be greater than in Rimini thanks to the complementary
 351 movable barrier system in use, which seals the port channel allowing to wall off the whole coastal perimeter,
 352 reducing the chance of water ingress in the urban area. In contrast, the erodible winter dune in the baseline
 353 defense scenario can only hold the heavy sea for shorter, less intense ESL events (RP 1 – 10 years), and becomes
 354 ineffective with more exceptional, long-lasting events; from 2050 on, the winter dune could be surmounted
 355 and dismantled by sea waves even during frequent events (RP 1 year).

356 **4.2 Expected Annual Damage**

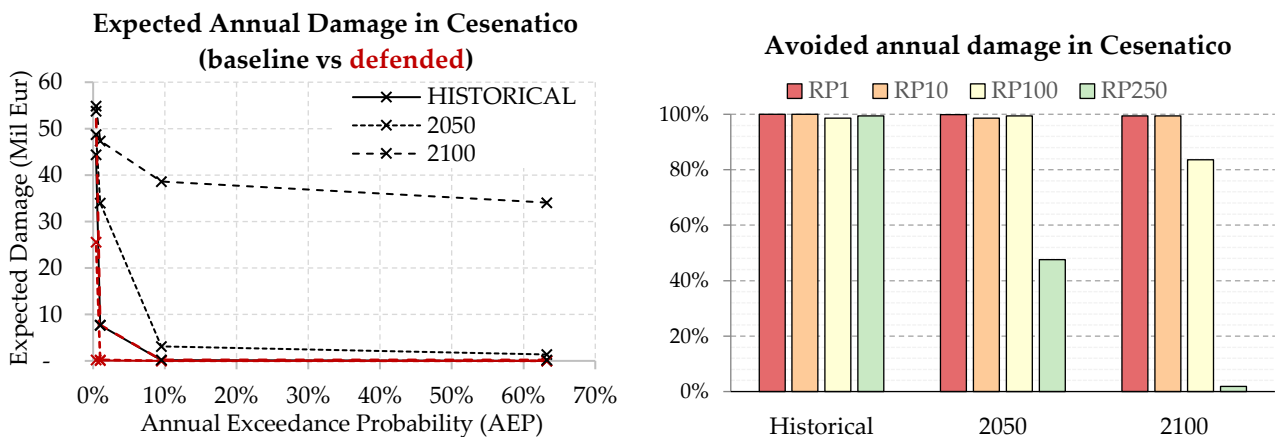
357 The Expected Annual Damage is calculated as a function of maximum exposed value and water depth. In
 358 Rimini, the EAD grows from around 650 thousand Eur under historical conditions to 2.8 million Eur in 2050
 359 and more than 32.3 million Eur in 2100. Under less severe ESL scenarios (RP below 100 years), the risk remains

360 mostly confined around the marina, which is located outside the defended area, producing an expected
 361 damage below 10 thousand Eur. Under more extreme ESL scenarios, the benefits of the *Parco del Mare* project
 362 protecting the southern part of Rimini become more evident, avoiding about 65% of the expected damages in
 363 the defended scenarios compared to the undefended ones. The damage avoided in the defended scenarios
 364 grow almost linearly with the increase of the baseline EAD under future projections of sea level rise: under
 365 the defended scenario, the EAD is reduced on average by 45% in comparison with the undefended scenario
 366 (figure 8, left). The project produces benefit up to scenario RP 250 years in 2100, where a projected TWL of 3.5
 367 meters would cause the overtopping of the barrier, reducing the benefits to almost zero (figure 8, right).



368
 369 **Figure 8.** Rimini: Expected Annual Damage (EAD) according to undefended scenario up to 2100, all town
 370 considered [left]; EAD reduction in the south-eastern part of the town thanks to hazard mitigation offered by
 371 the coastal barrier [right].

372 In Cesenatico, the average EAD for the undefended scenario grows from around 270 thousand Eur under
 373 historical conditions, to 1.7 million Eur in 2050 and almost 26 million Eur in 2100. In our simulations, the
 374 designed defence structure (a static barrier with height of 2.8 m along 7.8 km of coast) is able to avoid most of
 375 the damage inflicted to residential buildings (figure 9, left). The measure becomes less efficient for the most
 376 extreme scenarios in 2050 and 2100, when the increase in TWL causes the surmounting of the barrier (figure
 377 9, right). This assessment does not account for the impacts over those beach resorts and bathing facilities which
 378 are located along the barrier or between the barrier and the sea, and thus are equally exposed in both the
 379 baseline and the defended scenario; they would likely represent an additional 7-25% of the baseline damage.

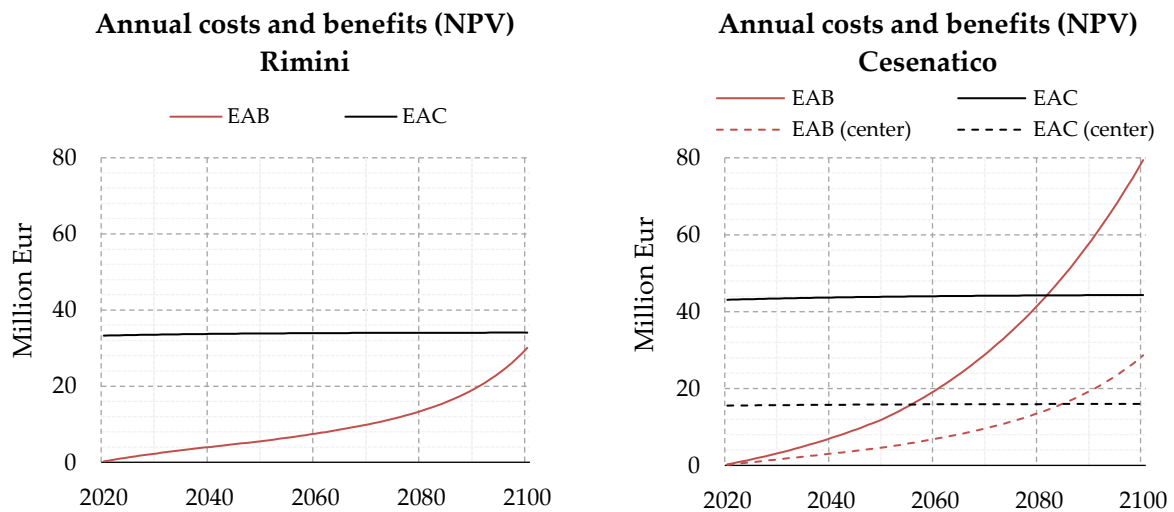


380
 381 **Figure 9.** Cesenatico: Expected Annual Damage (EAD) according to undefended scenario up to 2100 [left];
 382 EAD reduction thanks to hazard mitigation offered by the coastal barrier [right].

383 **4.3 Cost-Benefit Analysis**

384 The estimates of avoided direct flood impacts are accounted in a DRR-oriented CBA to evaluate the feasibility
385 of mitigation measures in terms of NPV, BCR and payback period for the two time-horizons (2021-2050: 30
386 years; and 2021-2100: 80 years). The assessment does not measure the indirect benefits brought in terms of
387 urban renovation, which are the primary focus of the *Parco del Mare* project, measuring, instead, only the direct
388 benefits in terms of direct flood damage reduction. In figure 10, the Expected Annual Benefits (EAB) grow at
389 faster rate approaching 2100 in both sites, because of the larger expected damages from more intense, less
390 frequent flood events. The cost of defence implementation is repaid by avoided damage after about 40 years
391 in Cesenatico and after 90 years in Rimini. At 2100, the BCR is 0.9 for Rimini and 1.8 for Cesenatico. These
392 results clearly indicate an overall profitability of the defence structure implementation over the long term for
393 Cesenatico. For the case of the municipality of Rimini, further investigation is required in order to account for
394 the non-DRR benefits of the seafront renovation project. For instance, the potential reduction in indirect losses
395 in terms of capital and labour productivity due to less frequent and less intense flooding events, and the
396 potential increase in tourism and well-being of citizens due to renewed urban landscape, are factors that could
397 be accounted for in a holistic CBA analysis and would likely return a shorter payback period.

398 In order to better understand the potential benefits of the mitigation measures over different areas of the two
399 municipalities, we compare the results in terms of CBR over a selection of exposed records corresponding to
400 the town higher-density area (i.e. Cesenatico historical center). Table 2 summarizes the metrics of the
401 assessment for different area extent selections. Results do not differ much when comparing the CBA over
402 different areas. In Cesenatico benefits grow proportionally to costs, so that the payback time does not change
403 when considering a section of the town or the whole coastal perimeter.



404

405 **Figure 10.** Cumulated flood defence costs and expected benefits at Net Present Value for Rimini (left) and
406 Cesenatico (right).

407

408

409 **Table 2.** Summary of CBA for planned or designed seaside defence project in Rimini (all town and south
 410 section only) and Cesenatico (all town and center only) over a time horizon of 30 and 80 years (2021 to 2050
 411 and 2021 to 2100).

Metrics	Rimini				Cesenatico			
	All town		South only		All town		Center only	
	2050	2100	2050	2100	2050	2100	2050	2100
Baseline EAD [M EUR]	2.8	32	0.5	14.6	1.7	25.9	0.5	12.4
Defended EAD [M EUR]	2.4	17	0.1	0.9	0.1	0.4	0.1	0.4
Expected Annual Benefits [M EUR]	0.3	15	0.4	13.7	1.6	25.5	0.4	11.9
Sum of EAB (discounted) [M EUR]	5.6	30	4.1	27.8	12.0	79.4	4.7	28.6
Sum of EAC (discounted) [M EUR]	33.8	34.0	33.8	34.0	43.8	44.3	15.8	16.0
Net Present Value [M EUR]	-28.3	-4.0	-29.8	-6.3	-31.8	35.1	-11.24	12.6
Benefit-Cost ratio [-]	0.16	0.88	0.12	0.81	0.28	1.79	0.30	1.79

412 5. Conclusion

413 In this study we addressed coastal inundation risk scenarios over two coastal towns located along the North
 414 Adriatic coastal plain of Italy, which is projected to become increasingly exposed to ESL events due to changes
 415 in MSL induced by SLR and local subsidence phenomena. Both locations are expected to suffer increasing
 416 economic losses from these events, unless effective coastal adaptation measures are put in place. To
 417 understand the upcoming impacts and the potential benefits of designed coastal projects, we run a CBA
 418 comparing the baseline and the defended scenario in terms of flood losses over residential buildings, which
 419 represent the largest share of exposed buildings' footprints (93%). The defended scenario accounts for the
 420 effect of a coastal barriers based on the design of *Parco del Mare*, an urban renovation project under construction
 421 in Rimini. The same type of defence structure is envisaged along the coastal perimeter of the nearby town of
 422 Cesenatico. First, we characterised reference ESL events in terms of frequency and intensity based on local
 423 historical observations; then, we projected ESL scenarios to 2050 and 2100, accounting for the combined effect
 424 of eustatic SLR and subsidence rates on the TWL, as obtained from existing local studies. We produced flood
 425 hazard maps estimating maximum flood extent and water depth using a high-resolution hydrodynamic model
 426 able to replicate the physics of the inundation process. The hazard maps were fed to a locally-calibrated
 427 damage model in order to calculate the expected annual damage for both baseline and defended scenarios. An
 428 increase in damage is expected for both urban areas from 2021 to 2100: in Cesenatico the EAD grows by a
 429 factor 96, in Rimini by a factor 49.

430 The results obtained from the CBA on both locations show growing profitability of present project investment
 431 over time, associated with the increase of damage triggered by intense ESL events: the EAD under the baseline
 432 hypothesis is expected to increase by 3.5-fold in 2050, up to 10-fold in 2100. The benefits brought by the coastal
 433 defence project become much larger in the second half of the century: the EAB grows 6.1-fold in Rimini, 6.5-
 434 fold in Cesenatico, from 2050 to 2100. Avoided losses are expected to match the project implementation costs
 435 after about 40 years in Cesenatico and 90 years in Rimini. Benefits are found to increase proportionally to costs;
 436 the payback period in Cesenatico is the same considering either an investment on the protection of the whole
 437 town or only part of it. Further assessments of these renovation projects should look to measure the indirect
 438 and spill-over effects over the local economy brought by the project, possibly accounting also for the intangible
 439 benefits and scenarios of exposure change. The results are calculated in relation to emission scenario RCP 4.5;
 440 compared to RCP 8.5 at 2050, the difference in SLR contribution is negligible (~0.05 m), while at 2100, the
 441 difference between the two emission scenarios is larger (around 0.2 m), thus additional scenario analysis is
 442 suggested in future research.

443 **Data availability**

444 Mattia Amadio, & Arthur H. Essenfelder. (2021). Coastal flood inundation scenarios over Cesenatico and
445 Rimini: hazard and risk for Business as Usual and Defended options [Data set]. Hosted by Zenodo:
446 <https://zenodo.org/record/4783443>

447 **Authors contribution**

448 MA, AHE and SB conceptualized the study and designed the experiments. AHE carried out the coastal hazard
449 modelling. SR advised the model setup and calculation. SB and PM provided required data and expertise
450 about the case study areas. MA performed the economic risk modelling and wrote the manuscript. SM
451 supported the CBA calculations. JM and SB managed the funding acquisition and project supervision. All co-
452 authors have reviewed the manuscript.

453 **Acknowledgment**

454 The research leading to this paper received funding through the projects CLARA (EU's Horizon 2020 research
455 and innovation programme under grant agreement 730482), SAFERPLACES (Climate-KIC innovation
456 partnership) and EUCP – European Climate Prediction system under grant agreement 776613. We want to
457 thank Luisa Perini for her kind support.

458 **References**

- 459 Amadio M, Scorzini AR, Carisi F, et al (2019) Testing empirical and synthetic flood damage models: the case
460 of Italy. *Nat Hazards Earth Syst Sci* 19:661–678. <https://doi.org/10.5194/nhess-19-661-2019>
- 461 Antonioli F, Anzidei M, Amorosi A, et al (2017) Sea-level rise and potential drowning of the Italian coastal
462 plains: Flooding risk scenarios for 2100. *Quat Sci Rev* 158:29–43.
463 <https://doi.org/10.1016/j.quascirev.2016.12.021>
- 464 Armaroli C, Ciavola P, Perini L, et al (2012) Critical storm thresholds for significant morphological changes
465 and damage along the Emilia-Romagna coastline, Italy. *Geomorphology* 143–144:34–51.
466 <https://doi.org/10.1016/j.geomorph.2011.09.006>
- 467 Armaroli C, Duo E (2018) Validation of the coastal storm risk assessment framework along the Emilia-
468 Romagna coast. *Coast Eng* 134:159–167. <https://doi.org/10.1016/j.coastaleng.2017.08.014>
- 469 ARPAE (2019) Relazione tecnica mappe della pericolosità e del rischio di alluvioni in ambito costiero
- 470 Boardman AE, Greenberg DH, Vining AR, Weimer DL (2018) *Cost-Benefit Analysis*. Cambridge University
471 Press
- 472 Bonaduce A, Pinardi N, Oddo P, et al (2016) Sea-level variability in the Mediterranean Sea from altimetry
473 and tide gauges. *Clim Dyn* 47:2851–2866. <https://doi.org/10.1007/s00382-016-3001-2>
- 474 Bos F, Zwaneveld P (2017) *Cost-Benefit Analysis for Flood Risk Management and Water Governance in the*
475 *Netherlands: An Overview of One Century*. SSRN Electron J. <https://doi.org/10.2139/ssrn.3023983>
- 476 Bouwer LM (2011) Have disaster losses increased due to anthropogenic climate change? *Bull Am Meteorol*
477 *Soc*. <https://doi.org/10.1175/2010BAMS3092.1>
- 478 Carbognin L, Teatini P, Tomasin A, Tosi L (2010) Global change and relative sea level rise at Venice: What
479 impact in term of flooding. *Clim Dyn* 35:1055–1063. <https://doi.org/10.1007/s00382-009-0617-5>
- 480 Carbognin L, Teatini P, Tosi L (2009) The impact of relative sea level rise on the Northern Adriatic Sea coast,
481 Italy. *WIT Trans Ecol Environ* 127:137–148. <https://doi.org/10.2495/RAV090121>

482 Carminati E, Martinelli G (2002) Subsidence rates in the Po Plain, northern Italy: the relative impact of
483 natural and anthropogenic causation. *Eng Geol* 66:241–255. [https://doi.org/10.1016/S0013-](https://doi.org/10.1016/S0013-7952(02)00031-5)
484 7952(02)00031-5

485 Church JA, White NJ (2011) Sea-Level Rise from the Late 19th to the Early 21st Century. *Surv Geophys*
486 32:585–602. <https://doi.org/10.1007/s10712-011-9119-1>

487 Ciavola P, Coco G (eds) (2017) *Coastal storms: processes and impacts*. Wiley-Blackwell

488 Comune di Rimini (2018) *Parco del Mare Sud - Strategia per la rigenerazione urbana*

489 Comune di Rimini (2019a) *Deliberazione originale di giunta comunale N. 99 del 11/04/2019*

490 Comune di Rimini (2019b) *Deliberazione originale di giunta comunale N. 118 del 02/05/2019*

491 Comune di Rimini (2020) *Deliberazione originale di giunta comunale N. 128 del 26/05/2020*

492 Comune di Rimini (2021a) *Deliberazione originale di giunta comunale N. 19 del 19/01/2021*

493 Comune di Rimini (2021b) *Deliberazione originale di giunta comunale N. 20 del 19/01/2021*

494 CRESME (2014) *Definizione dei costi di (ri)costruzione nell’edilizia*

495 Froehlich DC (2002) IMPACT Project Field Tests 1 and 2: “Blind” Simulation. 1–18

496 Gambolati G, Giunta G, Putti M, et al (1998) Coastal Evolution of the Upper Adriatic Sea due to Sea Level
497 Rise and Natural and Anthropic Land Subsidence. 1–34. <https://doi.org/10.1007/978-94-011-5147-4>

498 Garnier E, Ciavola P, Spencer T, et al (2018) Historical analysis of storm events: Case studies in France,
499 England, Portugal and Italy. *Coast Eng* 134:10–23. <https://doi.org/10.1016/j.coastaleng.2017.06.014>

500 Geofabrik GmbH (2018) *OpenStreetMap data extracts*

501 Hallegatte S, Green C, Nicholls RJ, Corfee-Morlot J (2013) Future flood losses in major coastal cities. *Nat*
502 *Clim Chang*. <https://doi.org/10.1038/nclimate1979>

503 Hinkel J, Lincke D, Vafeidis AT, et al (2014) Coastal flood damage and adaptation costs under 21st century
504 sea-level rise. *Proc Natl Acad Sci*. <https://doi.org/10.1073/pnas.1222469111>

505 Huizinga J, Moel H De, Szewczyk W (2017) *Global flood depth-damage functions : Methodology and the*
506 *Database with Guidelines*

507 IPCC (2019) *IPCC Special Report on the Ocean and Cryosphere in a Changing Climate*

508 ISPRA (2012) *Mare e ambiente costiero. Temat Primo Piano - Annu dei dati Ambient 2011 259–322*

509 ISTAT (2011) *15° censimento della popolazione e delle abitazioni*

510 Jongman B, Kreibich H, Apel H, et al (2012a) Comparative flood damage model assessment: towards a
511 European approach. *Nat Hazards Earth Syst Sci* 12:3733–3752

512 Jongman B, Ward PJ, Aerts JCJH (2012b) Global exposure to river and coastal flooding: Long term trends
513 and changes. *Glob Environ Chang*. <https://doi.org/10.1016/j.gloenvcha.2012.07.004>

514 Jonkman SN, Brinkhuis-Jak M, Kok M (2004) Cost benefit analysis and flood damage mitigation in the
515 Netherlands. *Heron* 49:95–111

516 Kain CL, Lewarn B, Rigby EH, Mazengarb C (2020) Tsunami Inundation and Maritime Hazard Modelling
517 for a Maximum Credible Tsunami Scenario in Southeast Tasmania, Australia. *Pure Appl Geophys*
518 177:1549–1568. <https://doi.org/10.1007/s00024-019-02384-0>

519 Kemp AC, Horton BP, Donnelly JP, et al (2011) Climate related sea-level variations over the past two
520 millennia. *Proc Natl Acad Sci U S A* 108:11017–11022. <https://doi.org/10.1073/pnas.1015619108>

521 Kind JM (2014) Economically efficient flood protection standards for the Netherlands. *J Flood Risk Manag*
522 7:103–117. <https://doi.org/10.1111/jfr3.12026>

- 523 Kirezci E, Young IR, Ranasinghe R, et al (2020) Projections of global-scale extreme sea levels and resulting
524 episodic coastal flooding over the 21st Century. *Sci Rep* 10:1–12. [https://doi.org/10.1038/s41598-020-](https://doi.org/10.1038/s41598-020-67736-6)
525 67736-6
- 526 Lambeck K, Antonioli F, Anzidei M, et al (2011) Sea level change along the Italian coast during the Holocene
527 and projections for the future. *Quat Int* 232:250–257. <https://doi.org/10.1016/j.quaint.2010.04.026>
- 528 Lambeck K, Purcell A (2005) Sea-level change in the Mediterranean Sea since the LGM: Model predictions
529 for tectonically stable areas. In: *Quaternary Science Reviews*. Pergamon, pp 1969–1988
- 530 Lionello P (2012) The climate of the Venetian and North Adriatic region: Variability, trends and future
531 change. *Phys Chem Earth* 40–41:1–8. <https://doi.org/10.1016/j.pce.2012.02.002>
- 532 Lionello P, Barriopedro D, Ferrarin C, et al (2020) Extremes floods of Venice: characteristics, dynamics, past
533 and future evolution. *Nat Hazards Earth Syst Sci* 1–34. <https://doi.org/10.5194/nhess-2020-359>
- 534 Lowe J (2008) Intergenerational wealth transfers and social discounting: Supplementary Green Book
535 guidance. HM Treasury, London 3–6
- 536 Lowe J, Gregory J, Flather R (2001) Changes in the occurrence of storm surges around the United Kingdom
537 under a future climate scenario using a dynamic storm surge model driven by the Hadley Centre
538 climate models. *Clim Dyn* 18:179–188
- 539 Marsico A, Lisco S, Lo Presti V, et al (2017) Flooding scenario for four Italian coastal plains using three
540 relative sea level rise models. *J Maps* 13:961–967. <https://doi.org/10.1080/17445647.2017.1415989>
- 541 Masina M, Lamberti A, Archetti R (2015) Coastal flooding: A copula based approach for estimating the joint
542 probability of water levels and waves. *Coast Eng* 97:37–52.
543 <https://doi.org/10.1016/j.coastaleng.2014.12.010>
- 544 McGranahan G, Balk D, Anderson B (2007) The rising tide: Assessing the risks of climate change and human
545 settlements in low elevation coastal zones. *Environ Urban*. <https://doi.org/10.1177/0956247807076960>
- 546 McInnes KL, Walsh KJE, Hubbert GD, Beer T (2003) Impact of sea-level rise and storm surges in a coastal
547 community. *Nat Hazards* 30:187–207. <https://doi.org/10.1023/A:1026118417752>
- 548 Mechler R (2016) Reviewing estimates of the economic efficiency of disaster risk management: opportunities
549 and limitations of using risk-based cost–benefit analysis. *Nat Hazards* 81:2121–2147.
550 <https://doi.org/10.1007/s11069-016-2170-y>
- 551 Meli M, Olivieri M, Romagnoli C (2021) Sea-level change along the Emilia-Romagna coast from tide gauge
552 and satellite altimetry. *Remote Sens* 13:1–26. <https://doi.org/10.3390/rs13010097>
- 553 Meyssignac B, Cazenave A (2012) Sea level: A review of present-day and recent-past changes and variability.
554 *J. Geodyn.* 58:96–109
- 555 Mitchum GT, Nerem RS, Merrifield MA, Gehrels WR (2010) Modern Sea-Level-Change Estimates. In:
556 *Understanding Sea-Level Rise and Variability*. Wiley-Blackwell, Oxford, UK, pp 122–142
- 557 Muis S, Verlaan M, Winsemius HC, et al (2016) A global reanalysis of storm surges and extreme sea levels.
558 *Nat Commun* 7:1–11. <https://doi.org/10.1038/ncomms11969>
- 559 Nicholls RJ, Cazenave A (2010) Sea-level rise and its impact on coastal zones. *Science* (80-) 328:1517–1520.
560 <https://doi.org/10.1126/science.1185782>
- 561 Olsen AS, Zhou Q, Linde JJ, Arnbjerg-Nielsen K (2015) Comparing methods of calculating expected annual
562 damage in urban pluvial flood risk assessments. *Water* (Switzerland) 7:255–270.
563 <https://doi.org/10.3390/w7010255>
- 564 Peltier WR (2004) Global Glacial Isostasy and the surface of the ice-age Earth: the ICE-5G (VM2) Model and
565 GRACE. *Annu Rev Earth Planet Sci* 32:111–149. <https://doi.org/10.1146/annurev.earth.32.082503.144359>

- 566 Peltier WR, Argus DF, Drummond R (2015) Space geodesy constrains ice age terminal deglaciation: The
567 global ICE-6G_C (VM5a) model. *J Geophys Res Solid Earth* 120:450–487.
568 <https://doi.org/10.1002/2014JB011176>
- 569 Perini L, Calabrese L, Deserti M, et al (2011) Le mareggiate e gli impatti sulla costa in Emilia-Romagna 1946-
570 2010
- 571 Perini L, Calabrese L, Lorito S, Luciani P (2015) Il rischio da mareggiata in Emilia-Romagna: l'evento del 5-6
572 Febbraio 2015. *Geol* 53:8–17
- 573 Perini L, Calabrese L, Luciani P, et al (2017) Sea-level rise along the Emilia-Romagna coast (Northern Italy) in
574 2100: Scenarios and impacts. *Nat Hazards Earth Syst Sci* 17:2271–2287. <https://doi.org/10.5194/nhess-17-2271-2017>
- 576 Perini L, Calabrese L, Salerno G, et al (2016) Evaluation of coastal vulnerability to flooding: Comparison of
577 two different methodologies adopted by the Emilia-Romagna region (Italy). *Nat Hazards Earth Syst Sci*
578 16:181–194. <https://doi.org/10.5194/nhess-16-181-2016>
- 579 Perini L, Calabrese L, Salerno G, Luciani P (2012) Mapping of flood risk in Emilia-Romagna coastal areas.
580 *Rend Online Soc Geol Ital* 21:501–502. <https://doi.org/10.13140/2.1.1703.7766>
- 581 Polcari M, Albano M, Montuori A, et al (2018) InSAR monitoring of Italian coastline revealing natural and
582 anthropogenic ground deformation phenomena and future perspectives. *Sustain* 10:4–7.
583 <https://doi.org/10.3390/su10093152>
- 584 Price R (2018) Cost-effectiveness of disaster risk reduction and adaptation to climate change. 1–21
- 585 Roberts S (2020) ANUGA - Open source hydrodynamic / hydraulic modelling
- 586 Roberts S, Nielsen O, Gray D, Sexton J (2015) ANUGA User Manual
- 587 Solari L, Del Soldato M, Bianchini S, et al (2018) From ERS 1/2 to Sentinel-1: Subsidence Monitoring in Italy
588 in the Last Two Decades. *Front Earth Sci* 6:. <https://doi.org/10.3389/feart.2018.00149>
- 589 Stocker TF, Dahe Q, Plattner G-K, et al (2013) Technical Summary. In: Stocker TF, Qin D, Plattner G-K, et al.
590 (eds) *Climate Change 2013: The Physical Science Basis. Contribution of Working Group I to the Fifth*
591 *Assessment Report of the Intergovernmental Panel on Climate Change*. Cambridge University Press,
592 Cambridge, United Kingdom and New York, NY, USA., pp 33–115
- 593 Syvitski JPM, Kettner AJ, Overeem I, et al (2009) Sinking deltas due to human activities. *Nat Geosci*.
594 <https://doi.org/10.1038/ngeo629>
- 595 Teatini P, Ferronato M, Gambolati G, et al (2005) A century of land subsidence in Ravenna, Italy. *Environ*
596 *Geol* 47:831–846. <https://doi.org/10.1007/s00254-004-1215-9>
- 597 Teatini P, Ferronato M, Gambolati G, Gonella M (2006) Groundwater pumping and land subsidence in the
598 Emilia-Romagna coastland, Italy: Modeling the past occurrence and the future trend. *Water Resour Res*
599 42:. <https://doi.org/10.1029/2005WR004242>
- 600 Tsimplis MN, Raicich F, Fenoglio-Marc L, et al (2012) Recent developments in understanding sea level rise at
601 the Adriatic coasts. *Phys Chem Earth* 40–41:59–71. <https://doi.org/10.1016/j.pce.2009.11.007>
- 602 Tsimplis MN, Rixen M (2002) Sea level in the Mediterranean Sea: The contribution of temperature and
603 salinity changes. *Geophys Res Lett* 29:51-1-51–4. <https://doi.org/10.1029/2002gl015870>
- 604 Umgiesser G, Bajo M, Ferrarin C, et al (2020) The prediction of floods in Venice: methods, models and
605 uncertainty. *Nat Hazards Earth Syst Sci* 1–47. <https://doi.org/10.5194/nhess-2020-361>
- 606 Vousdoukas MI, Mentaschi L, Feyen L, Voukouvalas E (2017) Extreme sea levels on the rise along Europe's
607 coasts. *Earth's Futur* 5:1–20. <https://doi.org/10.1002/ef2.192>
- 608 Vousdoukas MI, Mentaschi L, Voukouvalas E, et al (2018) Global probabilistic projections of extreme sea

609 levels show intensification of coastal flood hazard. Nat Commun 9:1–12. [https://doi.org/10.1038/s41467-](https://doi.org/10.1038/s41467-018-04692-w)
 610 018-04692-w

611 Wöppelmann G, Marcos M (2012) Coastal sea level rise in southern Europe and the nonclimate contribution
 612 of vertical land motion. J Geophys Res Ocean 117:. <https://doi.org/10.1029/2011JC007469>

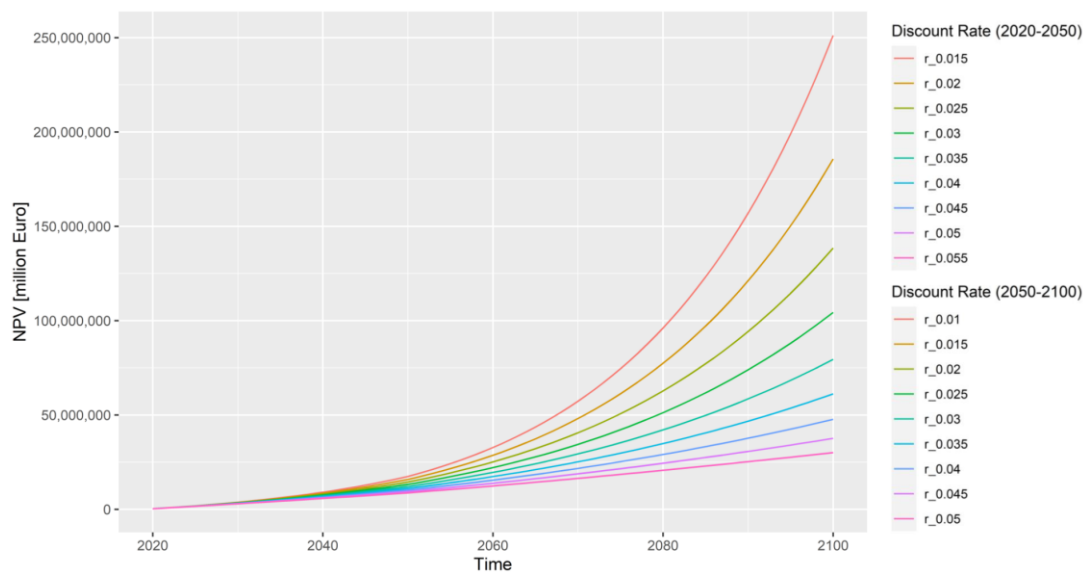
613 Zanchettin D, Bruni S, Raicich F, et al (2020) Review article: Sea-level rise in Venice: historic and future
 614 trends. Nat Hazards Earth Syst Sci Discuss 1–56. <https://doi.org/10.5194/nhess-2020-351>

615 Zanchettin D, Traverso P, Tomasino M (2007) Observations on future sea level changes in the Venice lagoon.
 616 Hydrobiologia. <https://doi.org/10.1007/s10750-006-0416-5>

617

618 **Annex 1**

619 A sensitivity analysis is carried out on the discount rate. Figure A1 below shows how the NPV changes with
 620 discount rate r ranging from 1.5% to 5.5% (2020 to 2050) and 1% to 5% (2050-2100).



621

622

Figure A1. Sensitivity analysis of NPV using a variable discount rate.